

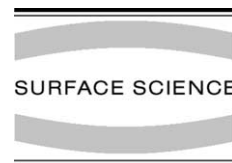


ELSEVIER

Available online at www.sciencedirect.com

SCIENCE @ DIRECT®

Surface Science 536 (2003) 55–60



www.elsevier.com/locate/susc

Homoepitaxial Ostwald ripening

M. Petersen ^{a,b}, A. Zangwill ^a, C. Ratsch ^{b,*}

^a School of Physics, Georgia Institute of Technology, Atlanta, GA 30332, USA

^b Department of Mathematics, UCLA, Los Angeles, CA 90095, USA

Received 21 January 2003; accepted for publication 11 April 2003

Abstract

This paper reports level set simulations of the Ostwald ripening of two-dimensional homoepitaxial islands. The simulation accurately accounts for both adatom diffusion between the islands and adatom attachment/detachment processes at the island edges. We compute the time evolution of the average island size and the full island size distribution function. The results provide support for a previously proposed self-consistent mean field theory.

© 2003 Elsevier Science B.V. All rights reserved.

Keywords: Diffusion and migration; Nucleation; Epitaxy; Growth; Computer simulations; Adatoms

In 1900, Wilhelm Ostwald published a famous paper on the approach to equilibrium for a solution where a dense phase and a dilute phase coexist [1]. When the dense phase is present in the form of a distribution of compact clusters with different sizes, he argued that the Gibbs–Thomson effect [2] provides a thermodynamic driving force for large clusters to grow at the expense of small clusters. This phenomenon is called ripening or coarsening. The basic physics is the desire of the system to minimize the free energy associated with the interfaces between the two phases. Sixty years later, Lifshitz and Sylozov and also Wagner (LSW) developed a theory of Ostwald ripening [3] which predicts that the cluster size distribution asymptotically evolves to a unique scaling form in the

limit when the dense phase volume fraction goes to zero. Contemporary theory takes account of transient effects and a finite volume fraction of the minority phase. Ref. [4] demonstrates that this theory can provide a very satisfactory account of experiment for three-dimensional (3D) bulk systems.

The study of Ostwald ripening in two dimensions (2D) became possible with the advent of ultra-high vacuum techniques in the 1960s. Using Auger and mass spectrometry, and field ion and transmission electron microscopy, a large effort was devoted to understanding the kinetics of thin film nucleation, growth, and coarsening. Solid clusters nucleate when deposited atoms diffuse across a flat, clean surface and collide with other diffusing atoms. During growth, subsequently deposited diffusing atoms either nucleate new clusters or collide with and adhere to existing clusters. Cluster ripening occurs when the deposition flux is turned off and the sample is held at fixed temperature. The early experiments gained much useful

* Corresponding author. Tel.: +1-310-825-4127; fax: +1-310-206-2679.

E-mail address: cratsch@math.ucla.edu (C. Ratsch).

information. However, the limited spatial resolution of the observations focused experimentation on systems where the deposited clusters took the form of easily visible three-dimensional crystallites [5,6]. This restriction introduces complications into the theory, particularly for heteroepitaxial systems where the three-dimensionality of the clusters is a consequence of lattice misfit elastic strain [7,8].

Most recently, scanning tunnelling microscopy (STM) and low-energy electron microscopy have made it possible to study Ostwald ripening for homoepitaxial systems where the clusters consist of one atom high islands. Examples include Si(001) [9], Ag(111) [10], Ni(100) [11], and TiN(100) and TiN(111) [12]. In principle, these experiments provide a quantitative test of theories of Ostwald ripening in 2D [13–17]. These theories are non-trivial because diffusion in 2D differs significantly from diffusion in 3D [18]. There are good experimental data for the time evolution of the average island size. The data for the asymptotic island size distribution function are less good. In practice, the experiments typically try to distinguish between two extreme limits of existing theory: ripening limited by surface diffusion and ripening limited by attachment/detachment of atoms to island edges. Of course, there is no guarantee that a given system conforms to either limit.

Based on its success for modelling epitaxial crystal growth [19], one might imagine that kinetic Monte Carlo (KMC) simulation would be a powerful tool to study 2D Ostwald ripening. In fact, we are aware of only a single paper devoted to this subject [20]. The reason is, for realistic values of the physical parameters, island detachment processes are so slow that good statistics require an inordinate amount of computer time. Consequently, simulationists tend to focus on coarsening by island diffusion and coalescence [21,22], a scenario that is known to occur for Ag(100) [23]. For reasons that are not entirely clear to us, the authors of Ref. [20] compared their simulation data to an analytic theory of coarsening by island diffusion [24], a process specifically disallowed in the simulations. Another approach that has been used to study Ostwald ripening is

based on the boundary integral method [31]. This method is extremely efficient for solving the diffusion equation (and hence island growth velocities) for a surface morphology in the absence of nucleation and merger.

In this paper, we study the Ostwald ripening of 2D homoepitaxial islands using the level set (LVST) approach to epitaxial phenomena [25–27]. This numerical method quantitatively reproduces the results of KMC growth simulations, including the detailed shape of the island size distribution in the submonolayer regime [28]. Moreover, LVST simulations are much more efficient than KMC simulations when island detachment processes are important [29]. The LVST method allows us to simulate nucleation and growth and subsequent coarsening within one unified approach, which is in contrast to the boundary integral method, where only the coarsening of islands can be simulated efficiently. In fact, in Ref. [31] the initial distribution of islands had to be specified by a separate simulation.

To our knowledge, the LVST method has been used once before to study 2D island coarsening [30]. In that work, Chopp digitized an STM image (to provide an initial condition) and reported LVST simulations which nicely reproduced STM images obtained during subsequent annealing. Quantitative agreement was obtained for the time evolution of the area of a single island in the field of view. In this paper, we are concerned with the *statistical* properties of 2D Ostwald ripening. Thus, we compute the time evolution of the entire island size distribution in addition to the time evolution of the (ensemble) average island size. We compare our size distribution with the analytic results of a self-consistent mean field theory of the ripening process in 2D [16].

In our implementation of the LVST method, islands are resolved as atomistic in height but continuous in the lateral dimensions. The boundaries of islands of height $k + 1$ are represented by the set of points \mathbf{x} where a level set function $\varphi(\mathbf{x}, t) = k$. The level set function evolves deterministically according to

$$\frac{\partial \varphi}{\partial t} + v_n |\nabla \varphi| = 0. \quad (1)$$

The normal velocity v_n is computed from an attachment flux and a detachment flux as

$$v_n = v^{\text{att}} - v^{\text{det}}. \quad (2)$$

Adatoms are represented by an adatom density which is updated by solving a diffusion equation. The attachment flux is [27]

$$v^{\text{att}} = a^2 D \left(\left. \frac{\partial \rho}{\partial n} \right|_{\text{terrace}} - \left. \frac{\partial \rho}{\partial n} \right|_{\text{top of island}} \right). \quad (3)$$

Here a is the lattice constant, D is the diffusion constant, and n the island boundary normal. The detachment flux is [29]

$$v^{\text{det}} = a^2 D_{\text{det}} p_{\text{esc}} \lambda, \quad (4)$$

where D_{det} is an effective detachment rate, p_{esc} is the probability that a detached particle escapes from the island, and λ is the density of particles that can detach from the island boundary. Explicit stochastic components of the calculation take proper account of the processes of island nucleation [28] and the dissociation of very small islands [29].

The main advantage of our approach is that it allows for rather large time steps during the simulation. The maximum allowable time step dt^{max} in a level set simulation is given by the condition

$$v_n dt^{\text{max}} < dx, \quad (5)$$

which says that a boundary cannot propagate more than one grid spacing during each time step. Since the growth rate of the ensemble averaged island size decreases monotonically with time during coarsening (cf. Fig. 1), the average of v_n also decreases monotonically. Thus, Eq. (5) implies that progressively larger time steps can be taken as the simulation advances.

Atoms were deposited onto the surface at constant deposition flux of 1 ML/s for all the results reported below. We chose $D/F = 10^6$ and $D_{\text{det}}/D = 0.001$ for, respectively, the ratio of the surface diffusion rate to the deposition flux and the ratio of the island edge detachment rate to the surface diffusion rate. Different choices for the physical parameters gave similar results. After exposing the substrate to an initial coverage Θ the deposition flux was turned off. Two coverages were considered, $\Theta = 0.085$ and $\Theta = 0.16$. In both cases

the simulations were carried out for a system of size 400×400 lattice constants represented on a numerical grid of 1132×1132 equidistant points. We report results for island radii R_i rather than island areas A_i to allow an easy comparison with the literature. For simplicity, we set $R_i = \sqrt{A_i/\pi}$. This is almost exact in our approach, particularly at coverages where island merger can be neglected.

For Ostwald ripening limited by adatom diffusion, a self-consistent mean field theory (MFT) described by Yao et al. [16] predicts that the average island radius \bar{R} increases as

$$\bar{R}(t) = [\bar{R}(t_0)^3 + K(\Theta)(t - t_0)]^{1/3}. \quad (6)$$

The predicted ripening exponent 1/3 depends on neither the coverage nor the dimensionality of the system. The function $K(\Theta)$ depends on both. In 2D, $K(\Theta)$ is predicted to diverge as $1/\ln \Theta^{-1/2}$ when $\Theta \rightarrow 0$.

The KMC simulation of 2D Ostwald ripening reported by Lam et al. [20] took account of exactly the same physical processes (adatom diffusion, edge atom detachment) used by us. However, their reported ripening exponents ($0.24 \leq \beta \leq 0.28$) fall somewhat below the MFT value. They suspected that their simulations may never have exited the transient regime.

Fig. 1 shows our LVST simulation results for the average island radius \bar{R} as a function of time for the two values of Θ noted above. After an initial transient phase, the data clearly approach the expected power law exponent at late times (see inset). Nevertheless, the effective exponents we extract from our late time data fall in the interval $0.28 \leq \beta \leq 0.30$. Thus, even with the increased efficiency of the level set method, our data do not quite reach asymptotic limit, at least as far as the mean island size is concerned. The scaling exponent has also been confirmed with the boundary integral method [31].

We note in passing that Eq. (6) is valid only for the case of adatom diffusion limited ripening. A KMC study by Mattsson et al. [21] showed that a significantly lower value for β (0.20–0.25) is obtained if ripening is primarily driven by island diffusion. We have not included this effect in the

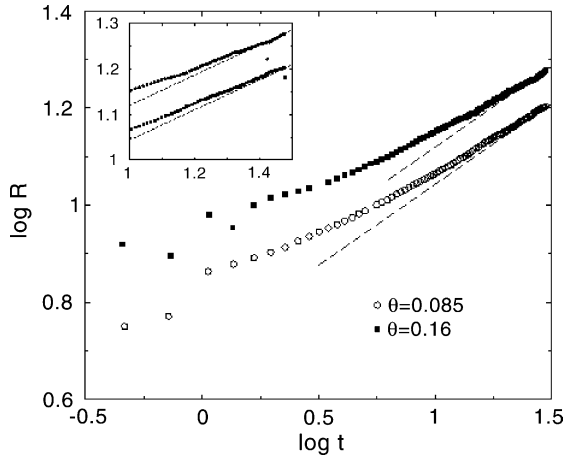


Fig. 1. Time dependence of the average island radius for two different coverages θ . The straight lines are guides to the eye with the theoretically predicted slope of $1/3$. Time is in seconds, and the radius is given in units of the lattice constant. The inset is a blow up of the asymptotic regime.

present work, but it is straightforward to do so without additional computational cost.

We now turn to our main result: the shape and time evolution of the scaled and normalized island size distribution function $g(z)$, where $z = R/\bar{R}$. In our LVST simulations we measure n_R , the number of islands with radius R . The MFT of Yao et al. predicts that $g(z) = n_R \bar{R}^3 \pi / \theta$ is independent of time, and that the shape of $g(z)$ depends only on the coverage θ [16]. Specifically, $g(z)$ broadens as θ increases.

Fig. 2 shows our LVST results for $g(z)$ for $\theta = 0.16$ and $\theta = 0.085$. It is evident that $g(z)$ scales very well; the data at different times collapse to a single curve for each coverage. Moreover, the width of $g(z)$ is indeed larger for $\theta = 0.16$ (lower panel of Fig. 2) than for $\theta = 0.085$ (upper panel of Fig. 2). Since both distributions are normalized to the same area (the total number of islands), this is obvious from the fact that the peak value of the $\theta = 0.16$ distribution is smaller than the peak value of the $\theta = 0.085$ distribution. A broadening of the size distribution with increasing θ has also been observed with the boundary integral method [31].

Significantly, we believe, the solid line in the upper panel shows that our $\theta = 0.085$ data agree

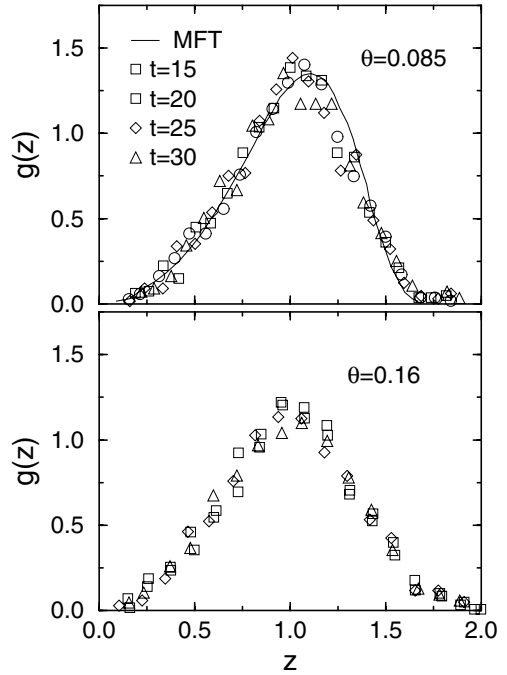


Fig. 2. Scaled island size distribution function $g(z)$ for $\theta = 0.085$ and $\theta = 0.16$. In each case, the distribution is shown at four different times. The MFT result is from Ref. [16].

very well with the mean field result for $g(z)$ derived by Yao et al. [16] for this coverage. The latter authors did not report a mean field prediction for $g(z)$ with $\theta = 0.16$ although it could be obtained (in principle) by a non-trivial numerical procedure outlined by them.

The scaled size distribution functions shown in Fig. 2 are independent of t for asymptotically large t . However, they may have a significantly different shape at earlier times. For example, during growth, the scaled island size distribution sharpens and narrows as the microscopic detachment rate D_{det} increases [29]. It is therefore instructive to study the time evolution of the size distribution in the pre-asymptotic regime. We present these data for $\theta = 0.16$ in Fig. 3. The distribution function quickly broadens and reaches its asymptotic shape at approximately $t \simeq 4$ s. We have checked (data not shown here) that the shape of $g(z)$ is independent of D_{det} at larger times (where the shape is converged), but that the time evolu-

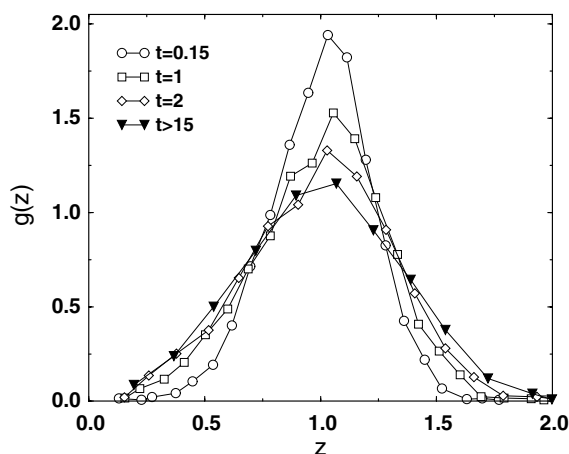


Fig. 3. Time evolution of the scaled island size distribution function $g(z)$ for $\theta = 0.16$.

tion to the asymptotic shape of the distribution function is different. A larger value of D_{det} leads to a sharper and narrower distribution function at the end of the growth phase, so it takes longer in the ripening phase for the distribution function to broaden.

In conclusion, we have used the numerically stable and efficient level set method to study nucleation and growth and subsequent Ostwald ripening in two dimensions within one computational framework. The computed time evolution of the average island size and the shape of the asymptotic scaled island size distribution agree quantitatively with the predictions of a previously published mean field theory of this process, as well as the results obtained from the boundary integral method. In retrospect, this confirmation is not unexpected because nucleation—the stochastic process which renders mean field theory unreliable for growth distributions, and makes the use of the boundary integral method numerically unfeasible—is absent during the ripening process.

Acknowledgements

MP was supported, in part, by the Department of Energy under grant DE-FG05-97ER45. We

also acknowledge support from the NSF focused research group grant DMS-0074152.

References

- [1] W. Ostwald, *Z. Phys. Chem.* 34 (1900) 495.
- [2] P. Pelcé, *Dynamics of Curved Fronts*, Academic, San Diego, 1988; See also J.G. McLean, B. Krishnamachari, D.R. Peale, E. Chason, J.P. Sethna, B.H. Cooper, *Phys. Rev. B* 55 (1997) 1811.
- [3] I.M. Lifshitz, V.V. Sylozov, *J. Phys. Chem. Solids* 19 (1961) 35; C. Wagner, *Z. Electrochem.* 65 (1961) 581.
- [4] J. Alkemper, V.A. Snyder, N. Akaiwa, P.W. Voorhees, *Phys. Rev. Lett.* 82 (1999) 2725.
- [5] J.A. Venables, G.D.T. Spiller, M. Hanbücken, *Rep. Prog. Phys.* 47 (1984) 399.
- [6] M. Zinke-Allmang, L.C. Feldman, M.H. Grabow, *Surf. Sci. Rep.* 16 (1992) 377.
- [7] I.V. Markov, *Crystal Growth for Beginners*, World Scientific, Singapore, 1995.
- [8] M. Iwamatsu, Y. Okabe, *J. Appl. Phys.* 86 (1999) 5541.
- [9] N.C. Bartelt, W. Theis, R.M. Tromp, *Phys. Rev. B* 54 (1996) 11741.
- [10] K. Morgenstern, G. Rosenfeld, G. Comsa, *Surf. Sci.* 441 (1999) 289.
- [11] M.S. Hoogeman, M.A.J. Klik, R. van Gastel, J.W.M. Frenken, *J. Phys. Cond. Mat.* 11 (1999) 4349.
- [12] S. Kodambaka, V. Petrova, A. Vailionis, P. Desjardins, D.G. Cahill, I. Petrov, J.E. Greene, *Thin Solid Films* 392 (2001) 164.
- [13] J.A. Marqusee, *J. Phys. Chem.* 81 (1984) 976.
- [14] Q. Zheng, J.D. Gunton, *Phys. Rev. A* 39 (1989) 4848.
- [15] T.M. Rogers, R.C. Desai, *Phys. Rev. B* 39 (1989) 11956.
- [16] J.-H. Yao, K.R. Elder, H. Guo, M. Grant, *Phys. Rev. B* 47 (1993) 14110.
- [17] B. Levitan, E. Domany, *Phys. Rev. E* 57 (1998) 1895.
- [18] R. Ghez, *A Primer of Diffusion Problems*, Wiley, New York, 1988.
- [19] Z. Zhang, M.G. Lagally, *Science* 276 (1997) 377.
- [20] P.-M. Lam, D. Bayayoko, X.-Y. Hu, *Surf. Sci.* 429 (1999) 161.
- [21] T.R. Mattsson, G. Mills, H. Metiu, *J. Chem. Phys.* 110 (1999) 12151.
- [22] A. Lo, R.T. Skodje, *J. Chem. Phys.* 112 (2000) 1966.
- [23] L. Bardotti, M.C. Bartelt, C.J. Jenks, C.R. Stoldt, J.-M. Wen, C.-M. Zhang, P.A. Thiel, J.W. Evans, *Langmuir* 14 (1998) 1487.
- [24] D. Kandel, *Phys. Rev. Lett.* 79 (1997) 4238.
- [25] M.F. Gyure, C. Ratsch, B. Merriman, R.E. Caffisch, S. Osher, J.J. Zinck, D.D. Vvedensky, *Phys. Rev. E* 58 (1998) R6927.
- [26] S. Chen, M. Kang, B. Merriman, R. Caffisch, C. Ratsch, R. Fedkiw, M. Gyure, S. Osher, *J. Comp. Phys.* 167 (2001) 475.

- [27] C. Ratsch, M.F. Gyure, R.E. Caflisch, F. Gibou, M. Petersen, M. Kang, J. Garcia, D.D. Vvedensky, *Phys. Rev. B* 65 (2002) 19503.
- [28] C. Ratsch, M.F. Gyure, S. Chen, M. Kang, D.D. Vvedensky, *Phys. Rev. B* 61 (2000) R10598.
- [29] M. Petersen, C. Ratsch, R.E. Caflisch, A. Zangwill, *Phys. Rev. E* 64 (2001) 061602.
- [30] D.L. Chopp, *J. Comp. Phys.* 162 (2000) 104.
- [31] N. Akaiwa, D.I. Meiron, *Phys. Rev. E* 51 (1995) 5408.